Acta Cryst. (1980). B**36**, 1525–1530

Structure of Partially Substituted Chlorapatite $(Ca,Sr)_5(PO_4)_3Cl$

BY K. SUDARSANAN AND R. A. YOUNG

Georgia Institute of Technology, Atlanta, Georgia 30332, *USA*

(*Received* 26 *June* 1979; *accepted* 22 *November* 1979)

Abstract

The structural location and effect of Sr partially substituting for Ca in chlorapatite, $Ca_5(PO_4)_3Cl$, have been determined from crystal structure refinements with X-ray data from three synthetic single crystals having Sr/Ca ratios from 0·02 to ~1·0. The crystals are all hexagonal with space group $P6_3/m$. When present in small amounts, Sr substitutes only for Ca(2) on the mirror plane but at a slightly different position, as accommodates its larger ion radius. With 48% replacement of Ca by Sr, 68% of the Ca(2) sites and 19% of the Ca(1) sites (on the threefold axis) were filled by Sr. The Cl atom shifts from 0,0,0·44 in chlorapatite to $0,0,\frac{1}{2}$, its position in $Sr_5(PO_4)_3Cl$, with increasing Sr content, dz/dA [where A is amount of Sr(2) present] being greatest initially. Vegard's law is obeyed within 2σ. The larger ion size and its preferential substitution on the border of the easy diffusion channel are the only observed features that could correlate with the known cariostatic effect of Sr in human tooth enamel or with the reported slight preferential loss of Sr that has replaced Ca in bone.

1. Introduction

Numerous studies have demonstrated that strontium ions can be incorporated into the mineral phase of skeletal tissue *in vivo* and into synthetic apatite and bone mineral *in vitro* (Baur, Carlsson & Lindqvist, 1961; Neuman & Neuman, 1958). The primary mechanism of this process has been described as hetero-ionic exchange, *e.g.* the displacement of Ca from its specific structural positions in the crystal to be replaced by Sr from the ambient soluble phase. The ability of teeth to concentrate ^{90}Sr has been used as a means of monitoring the extent of atomic fall-out (Starkey & Fletcher, 1969). Even with no contribution from fall-out, Sr is a constant trace element in teeth, though wide variations are found in the enamel of different teeth and the range varies from 25 to 600 p.p.m. in teeth from different geographic areas (Steadman, Brudevold & Smith, 1958). Caries examinations conducted in three Ohio communities, two of which had high levels of Sr and B in their drinking water and soil product (5·30 and 5·45 p.p.m. of Sr and 0·31 and 0·39 p.p.m. of B in water) and one of which contained low levels (0·20 p.p.m. of Sr and 0·04 p.p.m. of B in water), showed lower caries activity in the communities where drinking water contained a higher level of Sr and B (Curzon, Adkins, Bibby & Losee, 1970). Little & Barrett (1976*a*,*b*), from their studies of caries prevalence in the Atlantic Coast and West Coast areas of the USA, found that both F and Sr were incorporated in enamel at a statistically predictable level in the teeth of persons with little caries and that the enamels of people with low caries incidence had similar Sr compositions (300–400 p.p.m.).

Another point of biological interest is the slight preferential loss of Sr, over Ca, that has become incorporated in bone (Lengemann, 1957; Fig. 2 of Cohen & Gusanano, 1967).

A step toward understanding these effects of Sr presumably substituting for Ca in the biological apatite is determination of the detailed structural location and role of Sr substituting for Ca in the much simpler systems provided by synthetic apatites.

The structure of strontium hydroxide phosphate (strontium hydroxyapatite) has been reported in detail (Sudarsanan & Young, 1972); it is essentially the same as that of hydroxyapatite (Sudarsanan & Young, 1969). The strontium analogs differ from the calcium apatites in their crystallization characteristics under the same conditions. For example, octastrontium phosphate does not form under conditions suitable for the formation of octacalcium phosphate (Schnell, Kiesewetter, Kim & Hayek, 1971). Strontium chlorapatite differs structurally from the calcium analog in the position of chlorine. In $Sr_5(PO_4)_3Cl$ the Cl occurs at 0,0,0 and $0,0,\frac{1}{2}$, midway between the two Sr(2) triangles (Sudarsanan & Young, 1974), but in $Ca_5(PO_4)_3Cl$ the Cl occurs about 0·38 Å away, at 0,0,0·44 and 0,0,0·94 (Mackie, Elliott & Young, 1972). With the structural details of the two end members of the (Ca,Sr) apatite series known, a study of the mixed crystal warrants attention. In the biological context, it is the partial, rather than complete, substitutions which are of direct interest. Often the mixed-crystal structural details and properties cannot be obtained by simple interpolation

0567-7408/80/071525-06$01.00

from end-member properties. An example is the interaction of F, Cl and OH reported by Sudarsanan & Young (1978).

Ca ions in apatite occupy two non-equivalent positions. Ca(1) atoms are on the threefold axis at $\frac{1}{3},\frac{2}{3},z$ (where z is usually $<0{\cdot}01$) and three other equivalent sites and Ca(2) atoms on the mirror planes at $0{\cdot}01,0{\cdot}26,\frac{1}{4}$ and five other equivalent sites. Khudolozkin, Urusov & Tobelko (1972, 1973) and Urusov & Khudolozkin (1974) have shown from intensity measurements of X-ray powder patterns of solid solutions of (Ca,Sr) hydroxyapatite, at intervals of 20 mol%, and also from analysis of ordering energies that (i) Sr ions in (Ca,Sr) apatite occupy mainly Ca(2) sites in the apatite structure and (ii) the degree of ordering decreases almost linearly with increase in Sr content.

As a next step in characterizing the role of Sr in mixed apatites and, hence, its possible role in human dental enamel and bone, single-crystal X-ray structure refinements have been carried out for three apatites containing differing amounts of Sr.

2. Experimental

2.1. *Crystal growth*

Single crystals of (Ca,Sr) chlorapatite were prepared by standard flux-growth techniques (Prener, 1967). The starting material was calcium chlorapatite mixed with $CaCl_2$ and $SrCl_2$. The mixture was placed in a lightly covered platinum crucible and heated in a nitrogen atmosphere at 1553 K in a resistance furnace for 24 h. The furnace was cooled at the rate of 30 K per day to 1333 K, and then shut off. A nitrogen atmosphere was maintained at all elevated temperatures to exclude H_2O and CO_2. The resulting crystals were separated from the melt by being washed repeatedly in distilled hot water, then filtered out and dried. Crystals with hexagonal cross sections (maximum length ~4 mm and side 2 mm) were obtained. The calcium–strontium ratio was determined by atomic-absorption spectrometry. Crystals with three different calcium-to-strontium ratios were prepared (Table 1).

2.2. *Diffraction data*

For the X-ray studies, three spherical single-crystal specimens, designated *A*, *B* and *C*, of 0·22, 0·14, and 0·18 mm radius, respectively, were separately prepared from the products of the three different crystal-growth runs. Precession photographs showed that all three specimens have the space group $P6_3/m$. The lattice parameters for each crystal (Table 1) were determined on a Picker FACS-1 unit with 12 reflections, in the range from 70 to 110° (2θ), which were machine centered and used in a least-squares simultaneous refinement of the lattice parameters and orientation matrix.

Single-crystal X-ray reflection intensity data were determined with a Syntex $P2_1$ four-circle diffractometer equipped with a graphite monochromator, using Mo $K\alpha$ radiation, and operated in a routine θ–2θ continuous scan mode with scan rates from 29·3 to 2·9° min^{-1}. Stationary background counts were measured at the beginning ($B1$) and at the end ($B2$) of each scan with a total scan-to-background time ratio, TR, of 1·0. Intensities were calculated from the total scan count (CT) and background counts by the relation $I = [CT - (TR)(B1 + B2)] \times$ (scan rate). Absorption corrections were based on the tabular data in *International Tables for X-ray Crystallography* (1967) and the Ca/Sr ratio as determined by atomic-absorption spectroscopy (μR = 2·67, 0·46, and 0·80, respectively). The polarization corrections were made on the assumption that both the monochromator and the sample behaved as ideally mosaic crystals (Arndt & Willis, 1966; $2\theta = 12{\cdot}2°$ for the monochromator). Those reflections with intensities less than $2\sigma_c(I)$ (see σ_c definition below) were not included in the refinement. Half-normal probability plots tended to support the expectation that the bias thereby introduced (Hirshfeld & Rabinovich, 1973; Arnberg, Hovmöller & Westman, 1979) would not vitiate the main conclusions.

2.3. *Refinement of the structures*

Full-matrix least-squares refinements of all variable positional, temperature, site-occupancy and isotropic-secondary-extinction parameters were carried out with

Table 1. Sr *content and lattice parameters*

Crystal	Percentage Sr of (Sr + Ca) in the charge	by atomic absorption*	by site occupancy	a (Å)	c (Å)	Unit-cell volume (Å^3)
A	69·4	54·7	48·5 (6)	9·737 (2)	7·022 (4)	576·5
B	16·7	5·3	7·3 (2)	9·653 (3)	6·777 (1)	546·4
C	8·5	2·1	2·3 (2)	9·643 (1)	6·766 (1)	545·2
CaClAp				9·6418 (8)	6·7643 (2)	544·5
SrClAp				9·859 (1)	7·206 (2)	606·6

* Estimated precision based on repeated measurements is approximately 2% of the value shown.

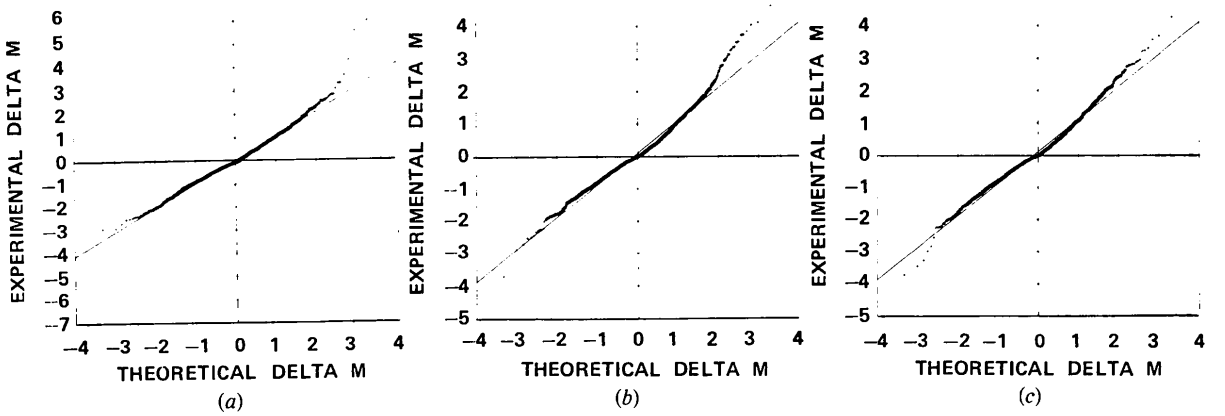

Fig. 1. Half-normal probability plots (δR type, Abrahams & Keve, 1971) with k in σ_x chosen best to nearest 0·01. (*a*) Crystal *A*, $k = 0{\cdot}04$, slope = 1·04; (*b*) crystal *B*, $k = 0{\cdot}055$, slope = 1·00; (*c*) crystal *C*, $k = 0{\cdot}07$, slope = 0·99.

Table 2. *R values and k in* σ_x

Crystal	Number of observations	R_1 (%)	R_2 (%)	K	wR_2 (%)	Σ_1
A	1080	6·2	6·9	0·04	8·1	1·07
				0·00	7·8	1·73
B	1133	3·2	3·9	0·055	7·2	1·04
				0·00	4·7	1·89
C	1147	5·5	6·8	0·07	11·3	1·04
				0·00	8·7	2·52

$$R_1 = \frac{\sum ||F_o| - |F_c||}{\sum |F_o|}, R_2 = \frac{\sum |F_o|^2 - |F_c|^2}{\sum |F_o|^2},$$

$$wR_2 = \left[\frac{\sum w(|F_o|^2 - |F_c|^2)^2}{\sum w|F_o|^4}\right]^{1/2}, \Sigma_1 = \left[\frac{\sum w(|F_o|^2 - |F_c|^2)^2}{N - P}\right]^{1/2},$$

where N = number of independent observations and P = number of parameters adjusted.

the *ORXFLS*3 program of Busing, Johnson, Ellison, Thiessen & Levy (1973). The sources of atomic-scattering factors used were Cromer & Waber (1965) for Sr^{2+}, Ca^{2+}, F^{1-} and Cl^{1-}, *International Tables for X-ray Crystallography* (1968) for O^{1-} and P^{1+}, the latter values being graphically extrapolated from those for P^0 with the help of the Si^0 and Si^{1+} difference. Anomalous-dispersion corrections were made with the values of f' and f'' calculated by Cromer (1965).

In the least-squares refinements, the weights used were reciprocal variances, $\sigma^2 = \sigma_c^2 + \sigma_x^2$, where σ_c, based on counting statistics, is given by $\sigma_c(I) = [CT + (TR)^2(B1 + B2)]^{1/2} \times$ (scan rate), and $\sigma_x = k|F|^2$ (Sudarsanan & Young, 1974). By trial and error, k was adjusted (in steps of 0·01 or, in one case, 0·005) to bring the best-straight-line slope of the half-normal probability plot (δR type, see Abrahams & Keve, 1971) to near unity (Fig. 1). Although addition of the σ_x term raised the wR_2 values significantly (Table 2) it is believed that the resulting larger calculated standard deviations are thereby brought closer to physical reality (Sudarsanan & Young, 1974). The resulting half-normal probability plots (produced in the last stages before the final cycle of refinement) are shown in Fig. 1. The purpose in producing these plots, and in adjusting σ_x to straighten them at the expense of increasing the σ's of the structural parameters, is to assure that we have not over-interpreted intensity data which are of only routine structure determination quality and not of precision structure refinement quality.

Initial refinements started from the strontium chlorapatite parameters (Sudarsanan & Young, 1974) for specimen *A*, in which there was the most strontium, and from chlorapatite parameters (Mackie *et al.*, 1972) for specimens *B* and *C*, in which there was more calcium than strontium. For specimens *B* and *C*, the refined site-occupancy factors and temperature parameters did not indicate any substitution of Sr for Ca(1) (on the threefold axis) whereas some substitution of Sr for Ca(2) (on the mirror planes) was indicated for all specimens. Initial refinements for specimen *A* showed that Sr was substituted for both Ca(1) and Ca(2). Subsequent refinements were therefore carried out with both Ca and Sr in the model. The following procedure was used to keep the refinement progressing in spite of the correlations between Sr and Ca. First, the overall scale factor was varied along with the variable positional and temperature parameters of all the atoms. Then, the site-occupancy factors of Ca(2) and Sr(2) were varied under the constraint that their sum be the stoichiometric value for the Ca(2) site. The Ca(2) and Sr(2) sites refined to different positions close to each other on the mirror planes at $z = \frac{1}{4}$ and $\frac{3}{4}$. For specimen *A*, which alone showed Sr substitution at the Ca(1) site, a similar constraint was introduced in refining the

site-occupancy factors for Sr(1) and Ca(1), during which the site-occupancy factors of all the other atoms were fixed at the stoichiometric values. In the next stage of refinement, the site-occupancy factors of all the atoms and their variable positional and temperature parameters were refined with the constraint on the site-occupancy factors for Ca(2) and Sr(2) atoms in all three cases and for Ca(1) and Sr(1) atoms also for specimen *A*.

For specimen *A*, in the process of refinement the Cl position moved so close to $0,0,\frac{1}{2}$ that further refinements could not be continued without assigning Cl to the special position at $0,0,\frac{1}{2}$. Therefore, Cl in specimen *A* was henceforth taken to be at $0,0,\frac{1}{2}$.

3. Results and discussion

The lattice parameters of the crystals are given in Table 1. As is shown by Fig. 2, Vegard's law is reasonably well obeyed, which gives one added confidence in the composition data obtained.

The final *R* factors are in Table 2 and the various structural parameters are given in Table 3.* In all three

* Lists of structure factors and anisotropic thermal parameters for crystals *A*, *B* and *C* have been deposited with the British Library Lending Division as Supplementary Publication No. SUP 35015 (23 pp.). Copies may be obtained through The Executive Secretary, International Union of Crystallography, 5 Abbey Square, Chester CH1 2HU, England.

Table 3. *Site-occupancy factors and positional parameters (multiplied by* 10^4*, except for fractions)*

	Crystal	Site-occupancy factor	*x*	*y*	*z*	*B* (Å²)*
O(1)	*A*	10000 (126)	3490 (4)	4952 (4)	$\frac{1}{4}$	1·26 (9)
	B	9698 (80)	3456 (2)	4935 (2)	$\frac{1}{4}$	0·93 (4)
	C	9821 (130)	3449 (3)	4929 (3)	$\frac{1}{4}$	0·77 (6)
	CaClAp		3436 (6)	4928 (5)	$\frac{1}{4}$	
	SrClAp		3365 (3)	4821 (3)	$\frac{1}{4}$	
O(2)	*A*	9627 (121)	5917 (3)	4636 (4)	$\frac{1}{4}$	1·41 (11)
	B	9646 (93)	5937 (1)	4652 (2)	$\frac{1}{4}$	0·80 (3)
	C	9996 (140)	5931 (3)	4656 (3)	$\frac{1}{4}$	0·72 (6)
	CaClAp		5927 (4)	4658 (5)	$\frac{1}{4}$	
	SrClAp		5861 (2)	4662 (3)	$\frac{1}{4}$	
O(3)	*A*	9332 (90)	3573 (4)	2721 (3)	739 (4)	1·11 (14)
	B	9841 (72)	3551 (1)	2685 (1)	670 (2)	0·79 (5)
	C	10000 (103)	3543 (3)	2676 (2)	673 (3)	0·59 (7)
	CaClAp		3542 (4)	2677 (3)	671 (5)	
	SrClAp		3549 (2)	2670 (2)	768 (2)	
P	*A*	9729 (60)	4100 (1)	3771 (1)	$\frac{1}{4}$	0·51 (2)
	B	10000 (35)	4090 (1)	3763 (0)	$\frac{1}{4}$	0·49 (2)
	C	9822 (61)	4083 (1)	3757 (1)	$\frac{1}{4}$	0·29 (2)
	CaClAp		4078 (1)	3754 (1)	$\frac{1}{4}$	
	SrClAp		4052 (1)	3720 (1)	$\frac{1}{4}$	
Ca(1)	*A*	8060 (48)	$\frac{1}{3}$	$\frac{2}{3}$	20 (2)	0·64 (2)
	B	9604 (47)	$\frac{1}{3}$	$\frac{2}{3}$	34 (1)	0·61 (2)
	C	9610 (60)	$\frac{1}{3}$	$\frac{2}{3}$	34 (1)	0·47 (2)
	CaClAp		$\frac{1}{3}$	$\frac{2}{3}$	38 (2)	
Sr(1)	*A*	1927 (48)	$\frac{1}{3}$	$\frac{2}{3}$	2 (1)	0·64 (2)
	B	–	–	–	–	
	C	–	–	–	–	
	SrClAp		$\frac{1}{3}$	$\frac{2}{3}$	4 (1)	
Ca(2)	*A*	3205 (7)†	−26 (6)	2535 (6)	$\frac{1}{4}$	0·62 (2)
	B	8257 (34)	−62 (3)	2543 (3)	$\frac{1}{4}$	0·62 (2)
	C	9190 (33)	−51	2547	$\frac{1}{4}$	0·46 (2)
	CaClAp		−52 (1)	2544 (1)	$\frac{1}{4}$	
Sr(2)	*A*	6782 (37)	123 (1)	2595 (1)	$\frac{1}{4}$	0·62 (2)
	B	1160 (34)†	80 (10)	2530 (12)	$\frac{1}{4}$	0·62 (2)
	C	359 (33)†	94 (22)	2510 (11)	$\frac{1}{4}$	0·46 (2)
	SrClAp		104 (1)	2592 (1)	$\frac{1}{4}$	
Cl	*A*	9262 (90)	0	0	$\frac{1}{2}$	1·48 (5)
	B	9484 (99)	0	0	4633 (2)	1·45 (4)
	C	9301 (116)	0	0	4508 (4)	1·06 (4)
	CaClAp		0	0	4438 (6)	
	SrClAp		0	0	$\frac{1}{2}$	

* These are 'equivalent' isotropic values calculated after the fact from the actually refined anisotropic thermal parameters, which have been deposited.

† These e.s.d.'s are not independent; Ca(2) and Sr(2) site occupancies were constrained as discussed in the text.

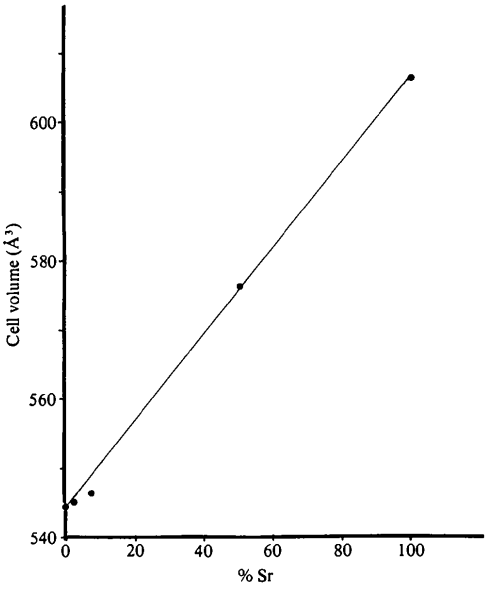

Fig. 2. Unit-cell volume as a function of composition.

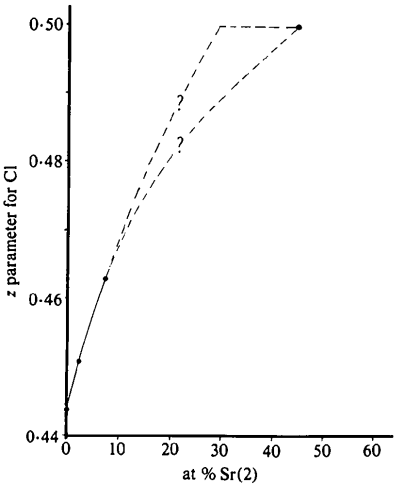

Fig. 3. Dependence of Cl position on amount of Sr(2) present. The two dashed lines show the range within which reasonable interpolations between the last two points could lie; from the results in hand there is no reason to preclude the possibility that the Cl could be moved to the more symmetric position, $z = 0{\cdot}50$, by substantially less Sr than that in specimen *A*.

crystals, the PO_4 groups and the cations (Ca & Sr) occupy much the same structural locations as they do in stoichiometric apatites.

The site-occupancy factors given can be taken as relative measures of the various atoms present in the different specimens. The site-occupancy data for Sr compare favorably with the amounts indicated as present by atomic-absorption spectrometry (Table 1). This agreement gives one some confidence that the boot-strapping procedure used to obtain the Sr site occupancies, in the presence of Ca at essentially the same sites, did lead to valid results. The site occupancies initially found for oxygens in specimens *B* and *C* were more than the stoichiometric value. The site-occupancy factors for all atoms listed in Table 3 for these two specimens are values normalized to give a stoichiometric value (1·00) for the site-occupancy factor for the atom in the PO_4 group which showed the highest value in that specimen. Specimens *B* and *C* appear to be (Ca,Sr) deficient.

Refinements carried out with a distribution of dummy atoms equally spaced along the *c* axis did not show major scattering density at any positions other than those given in Table 3.

There are two Sr-concentration-dependent effects noted:

(1) There is a preferential substitution of Sr at the Ca(2) sites. This effect is especially dominant for low concentrations of Sr. In specimens *B* and *C*, which contain 7·3 and 2·3% Sr (expressed as percentages of the total site-occupancy factors), there is no substitution at the Ca(1) site. But in specimen *A*, which contains 48% Sr, ~68% of the Ca(2) sites and ~19% of the Ca(1) sites are occupied by Sr.

(2) The chlorine position is also found to be dependent on the amount of Sr present, shifting from 0,0,0·44 in Ca chlorapatite to 0,0,$\frac{1}{2}$ (the position in Sr chlorapatite) when or before 48% of the Ca is replaced by Sr (Fig. 3). Since it is Sr(2) and not Sr(1) that borders the column of Cl ions at 0,0,*z*, one expects the amount of Sr(2), not total Sr, to be the factor affecting the Cl position. Fig. 3 shows the indicated dependence of Cl position on Sr(2) content. The few data points do seem to suggest a curve with steepest slope at the outset, as would be expected, and reaching $z = \frac{1}{2}$ at or before the Sr(2)-for-Ca(2) replacement reaches 48%.

We thank D. W. Holcomb for the atomic-absorption data, Professor J. A. Bertrand for this trial use of the Syntex $P2_1$ diffractometer, Dr D. G. Vanderveer for assistance in collecting the intensity data and the US Public Health Service for financial support through NIH-NIDR Grant DE-01912.

References

ABRAHAMS, S. C. & KEVE, E. T. (1971). *Acta Cryst.* A**27**, 157–164.

ARNBERG, L., HOVMÖLLER, S. & WESTMAN, S. (1979). *Acta Cryst.* A**35**, 497–499.

ARNDT, U. W. & WILLIS, B. T. M. (1966). *Single-Crystal Diffractometry*, p. 286. Cambridge Univ. Press.

BAUR, G. C. H., CARLSSON, A. & LINDQVIST, B. (1961). *Metabolism and Homeostatic Function of Bone in Mineral Metabolism*, Vol. 1, pp. 609–676. New York: Academic Press.

BUSING, W. R., JOHNSON, C. K., ELLISON, R. D., THIESSEN, W. E. & LEVY, H. A. (1973). *ORXFLS3. World List of Crystallographic Computer Programs*, 3rd ed., Accession No. 84. *J. Appl. Cryst.* **6**, 309–346.
COHEN, S. H. & GUSANANO, E. A. (1967). *Proc. Soc. Exp. Biol. Med.* **126**, 79–83.
CROMER, D. T. (1965). *Acta Cryst.* **18**, 17–23.
CROMER, D. T. & WABER, J. T. (1965). *Acta Cryst.* **18**, 104–109.
CURZON, M. E. J., ADKINS, B. L., BIBBY, B. G. & LOSEE, F. L. (1970). *J. Dent. Res.* **49**, 526–528.
HIRSHFELD, F. L. & RABINOVICH, D. (1973). *Acta Cryst.* A**29**, 510–513.
International Tables for X-ray Crystallography (1967). Vol. II, 2nd ed. Birmingham: Kynoch Press.
International Tables for X-ray Crystallography (1968). Vol. III, 2nd ed. Birmingham: Kynoch Press.
KHUDOLOZKIN, V. O., URUSOV, V. S. & TOBELKO, K. I. (1972). *Geochem. Int.* **9**, 827–833.
KHUDOLOZKIN, V. O., URUSOV, V. S. & TOBELKO, K. I. (1973). *Geochem. Int.* **10**, 266–269.
LENGEMANN, F. W. (1957). *Proc. Soc. Exp. Biol. Med.* **94**, 64–66.
LITTLE, M. F. & BARRETT, K. (1976*a*). *Caries Res.* **10**, 297–307.
LITTLE, M. F. & BARRETT, K. (1976*b*). *Arch. Oral Biol.* **21**, 651–657.
MACKIE, P. E., ELLIOTT, J. C. & YOUNG, R. A. (1972). *Acta Cryst.* B**28**, 1840–1848.
NEUMAN, W. R. & NEUMAN, M. W. (1958). *The Chemical Dynamics of Bone Mineral.* Chicago Univ. Press.
PRENER, J. S. (1967). *J. Electrochem. Soc.* **114**, 77–83.
SCHNELL, E., KIESEWETTER, W., KIM, Y. H. & HAYEK, E. (1971). *Monatsh. Chem.* **102**, 1327–1336.
STARKEY, W. E. & FLETCHER, W. (1969). *Arch. Oral Biol.* **14**, 169–179.
STEADMAN, L. T., BRUDEVOLD, F. & SMITH, F. A. (1958). *J. Am. Dent. Assoc.* **57**, 340–344.
SUDARSANAN, K. & YOUNG, R. A. (1969). *Acta Cryst.* B**25**, 1534–1543.
SUDARSANAN, K. & YOUNG, R. A. (1972). *Acta Cryst.* B**28**, 3668–3670.
SUDARSANAN, K. & YOUNG, R. A. (1974). *Acta Cryst.* B**30**, 1381–1386.
SUDARSANAN, K. & YOUNG, R. A. (1978). *Acta Cryst.* B**34**, 1401–1407.
URUSOV, V. S. & KHUDOLOZKIN, V. O. (1974). *Geochem. Int.* **11**, 1048–1053.

Acta Cryst. (1980). B**36**, 1530–1536

Multicomponent Polyanions. 28. The Structure of $K_7Mo_8V_5O_{40}\cdot\sim 8H_2O$, a Compound Containing a Structurally New Potassium-Coordinated Octamolybdopentavanadate Anion

BY ARNE BJÖRNBERG

Department of Inorganic Chemistry, University of Umeå, S-901 87 Umeå, Sweden

(*Received* 6 *December* 1979; *accepted* 12 *March* 1980)

Abstract

The crystal structure of $K_7Mo_8V_5O_{40}\cdot\sim 8H_2O$ has been determined from X-ray diffraction data collected with a Syntex $P2_1$ automatic four-circle diffractometer and Mo $K\alpha$ radiation. The monoclinic ($P2_1/n$) unit cell has $a = 19{\cdot}435\ (4)$, $b = 20{\cdot}237\ (5)$, $c = 12{\cdot}769\ (3)$ Å, $\beta = 108{\cdot}29\ (2)°$, $Z = 4$. The structure was refined to R 0·070 based on 7418 independent reflexions. The structure is built up from $[Mo_8V_5O_{40}]^{7-}$ anions which are linked together by K^+ ions and water molecules in a three-dimensional framework. The anion consists of edge-sharing MoO_6 octahedra forming an eight-membered ring in a two-up–two-down fashion. VO_5 trigonal bipyramids fill the gaps between the pairs of octahedra, and the fifth V atom is found in a VO_4 tetrahedron in the center of the anion, which within experimental error possesses $\bar{4}$ symmetry. For edge-sharing polyhedra the Mo—Mo distances vary between 3·302 (2) and 3·377 (2) Å, and the Mo—V distances between 3·426 (3) and 3·524 (3) Å. The Mo—O distances within the octahedra are 1·680 (11)–2·386 (10) Å. The VO_5 trigonal bipyramids all have one extremely long V—O distance (>2·7 Å). There is a K^+ ion situated in the large void at each of the two sides of the anion ring, coordinating eight anion O atoms which form a bi-peaked hexagonal pyramid. The remaining five K^+ ions all coordinate 5–8 anion and water O atoms.

Introduction

The interpretation of data from potentiometric EMF measurements in the system H^+—MoO_4^{2-}—HVO_4^{2-} is difficult due to the formation of several different

0567-7408/80/071530-07$01.00